Investigations & Properties of Parametric X-Ray Radiation

Исследования & свойства параметрического рентгеновского излучения

A.V. Shchagin,
Kharkov Institute of Physics and Technology, Kharkov 61108, Ukraine
shchagin@kipt.kharkov.ua

XL Winter School PINP, S. Petersburg, Russia, February 2006

21 year of experimental discovery of PXR Tomsk 1985

- **First theoretical predictions**

- Ya. B. Fainberg, N.A. Khizhnyak JETP 1957
- M.L. Ter-Mikaelian, book, 1969 – X-rays
- V.G. Baryshevsky, I.D. Feranchuk; G.M. Garibian, C. Yang - Dynamical theory -1970

Some reviews about PXR properties and investigations

1. **M.L. Ter-Mikaelian, *Electromagnetic radiation processes in periodic media at high energies,* Uspekhi Fizicheskikh Nauk, 171, 597-624 (2001) [in Russian]. Physics-Uspekhi 44, 571-596 (2001) [in English].**

2. **A.V. Shchagin, X.K. Maruyama, *Parametric X-rays,* in: Accelerator-based atomic physics technique and applications, eds. S.M. Shafroth, J.C. Austin (AIP Press, New York, 1997) pp. 279-307.**

3. **Rullhusen, A. Artru, P. Dhez, *Novel radiation sources using relativistic electrons,* World Scientific Publishers, Singapore, 1998.**

4. **A.V. Shchagin, *Investigations and properties of PXR,* in: Electron-photon interactions in dense media, ed. by H. Wiedemann, NATO Science Series, II Mathematics, Physics and Chemistry, Vol. 49, Kluwer Academic Publishers, Dordrecht/Boston/London, 2002, pp. 133-151.**

Схема Гюйгенса для излучения Вавилова-Черенкова

Fig

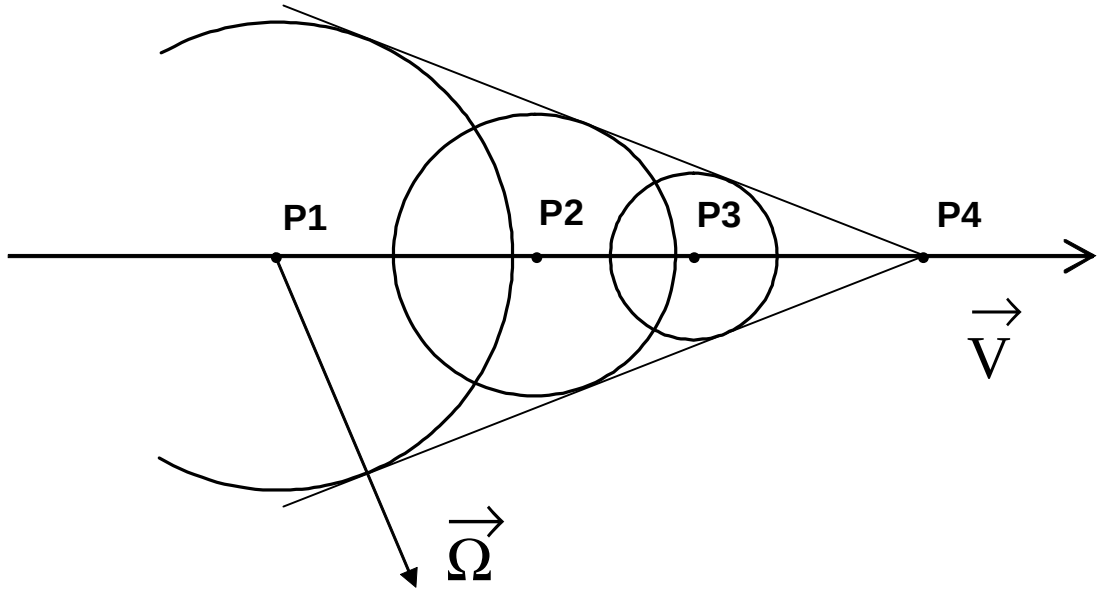

Рис. 1.1. Схема Гюйгенса для излучения Вавилова-Черенкова. Заряженная частица движется в однородной среде со скоростью $|\vec{V}| > \frac{c}{\sqrt{\varepsilon}}$. Сферические волны излучения, возбуждаемого частицей в среде, распространяются из точек P1-P3, произвольно расположенных вдоль траектории частицы. Излучение Вавилова-Черенкова распространяется вдоль вектора $\vec{\Omega}$

The Huygens construction for generation of PXR

Fig

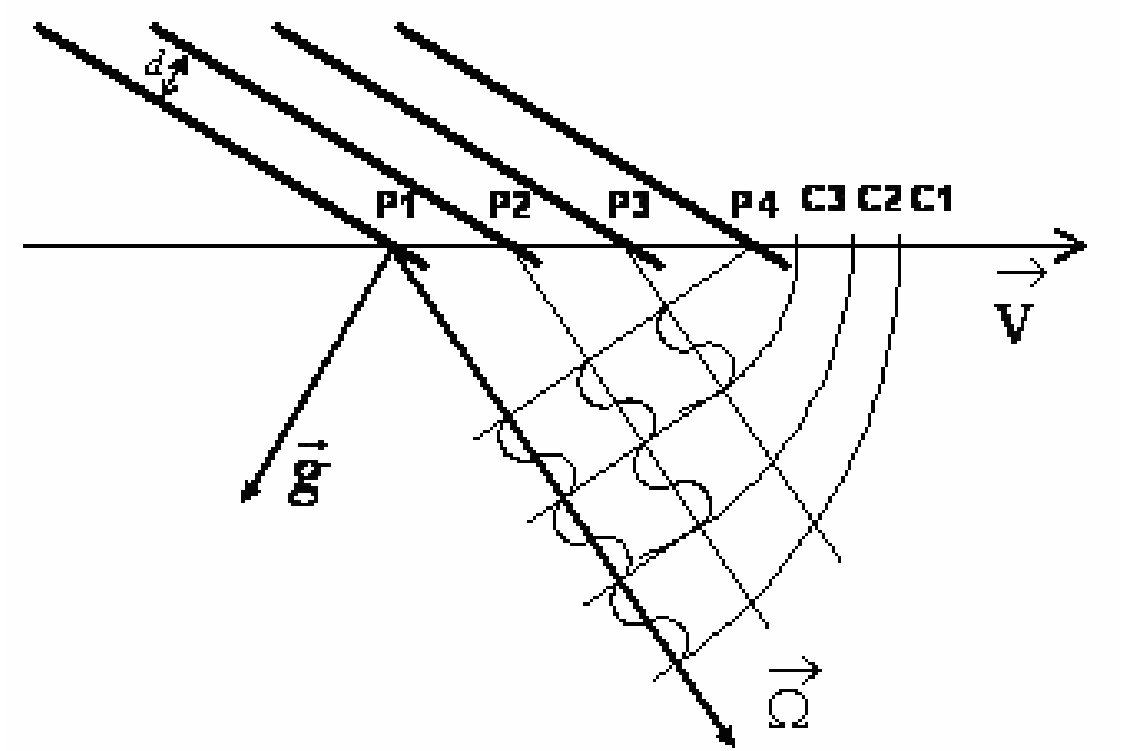

$$E_{CR} = \mathbf{h} \cdot w_{CR} = n_1 \cdot \frac{c \cdot \mathbf{h} \cdot \left| \vec{g} \cdot \vec{V} \right|}{c - \sqrt{e_0} \cdot \vec{V} \cdot \vec{\Omega}}$$

PXR as a diffraction of virtual photons

Fig

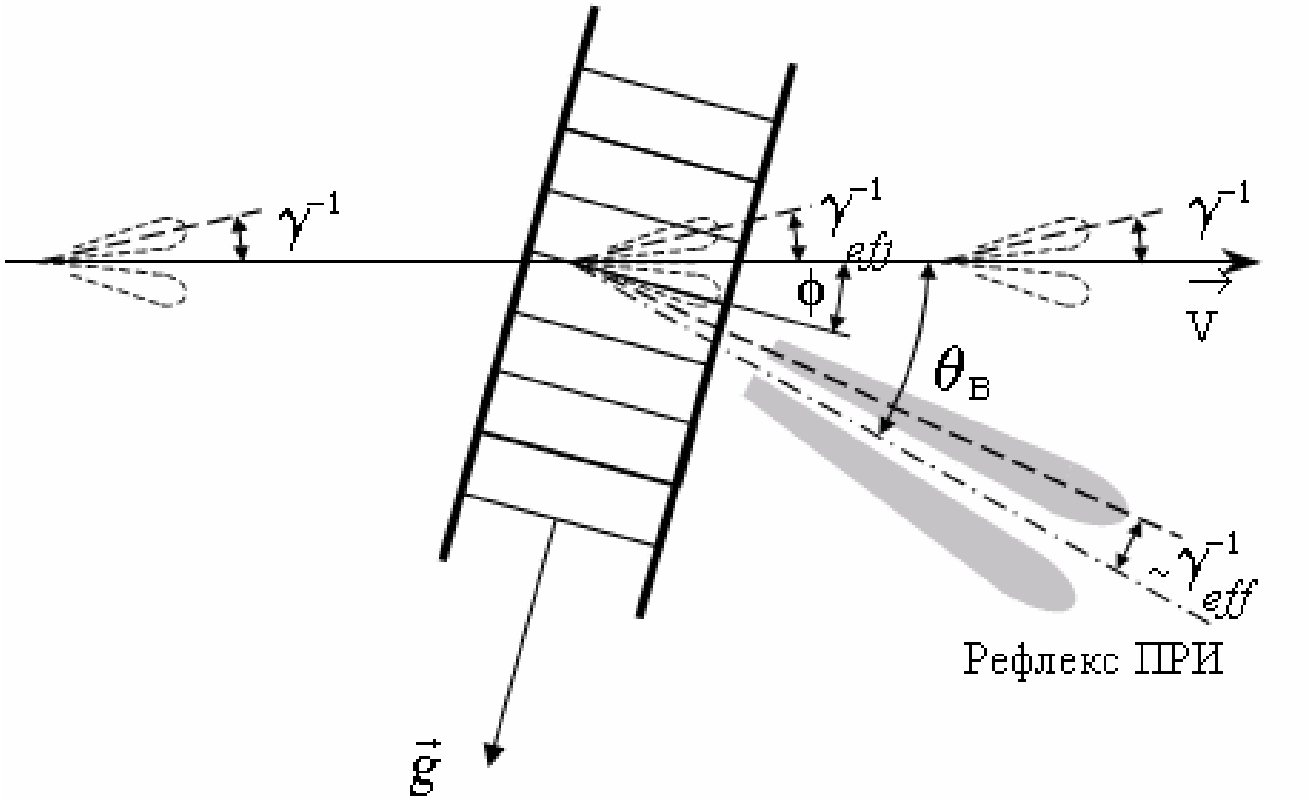

Common schemes for generation of PXR

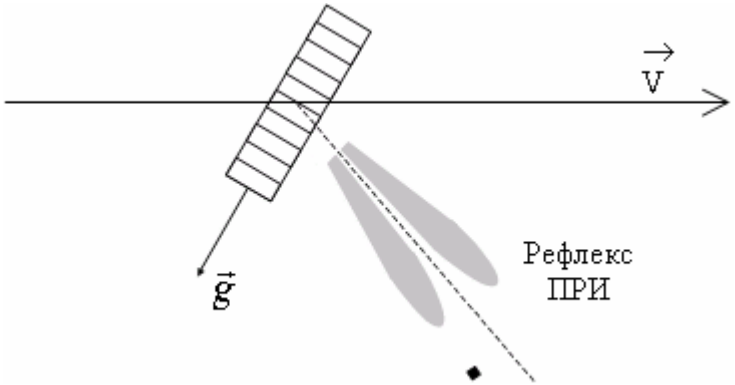

Laue geometry

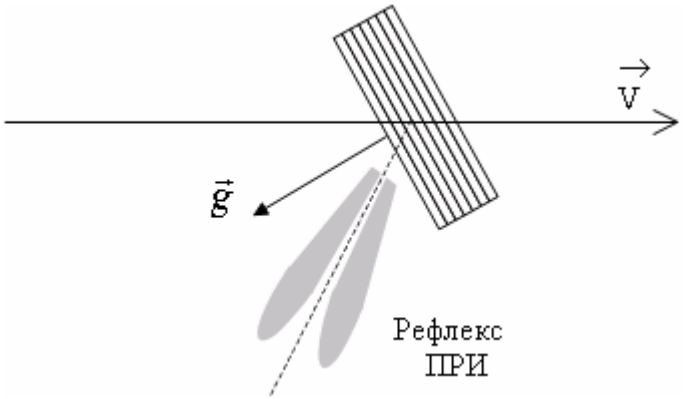

Bragg geometry

Измерение дифференциальных свойств PXR.

Схема экспериментальной установки с энергией пучка электронов 15.7-25.7 МэВ.

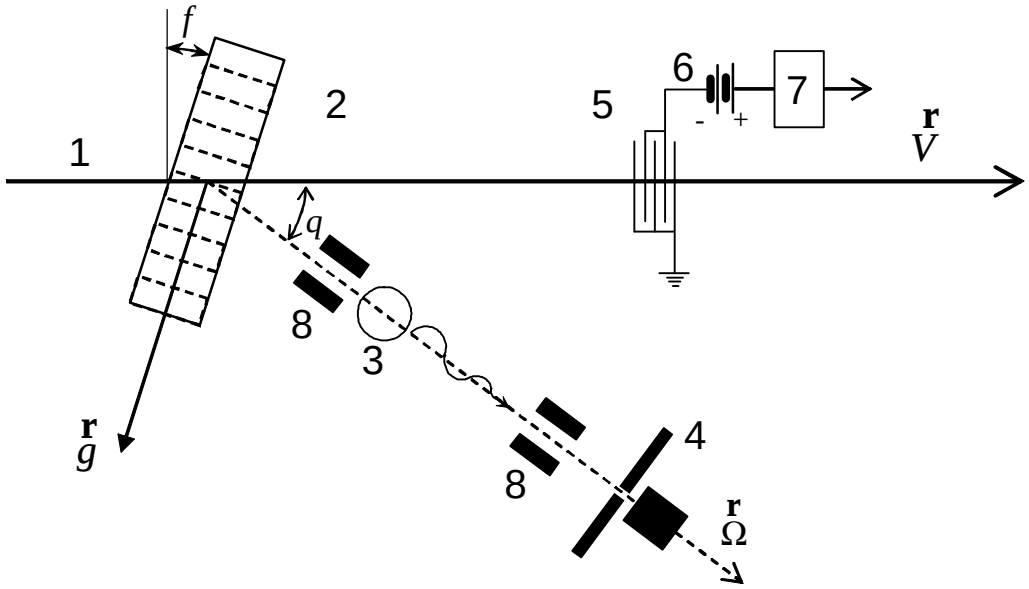

Эффективная площадь регистрации Si(Li) детектора рентгеновского излучения со свинцовой диафрагмой диаметром 3.7 мм

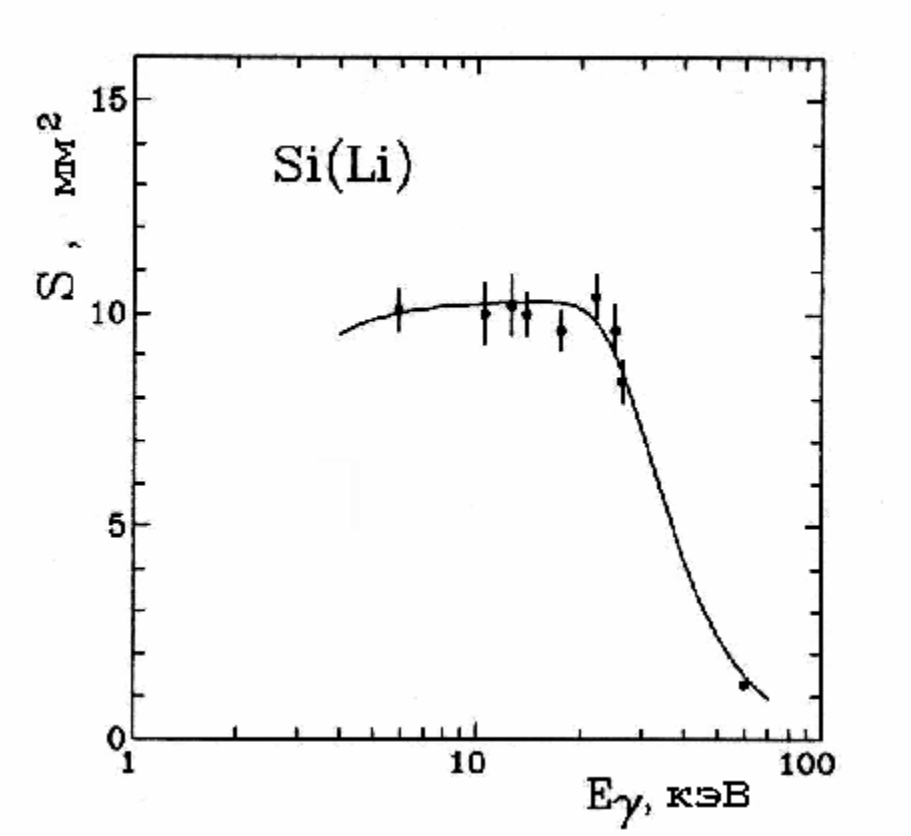

Спектр рентгеновского излучения измеренный при 142.9 мрад и энергии электронов 25.0 МэВ из монокристалла Si

Shchagin A.V., Pristupa V.I., Khizhnyak N.A. Phys. Lett. A 148, 485-488 (1990).

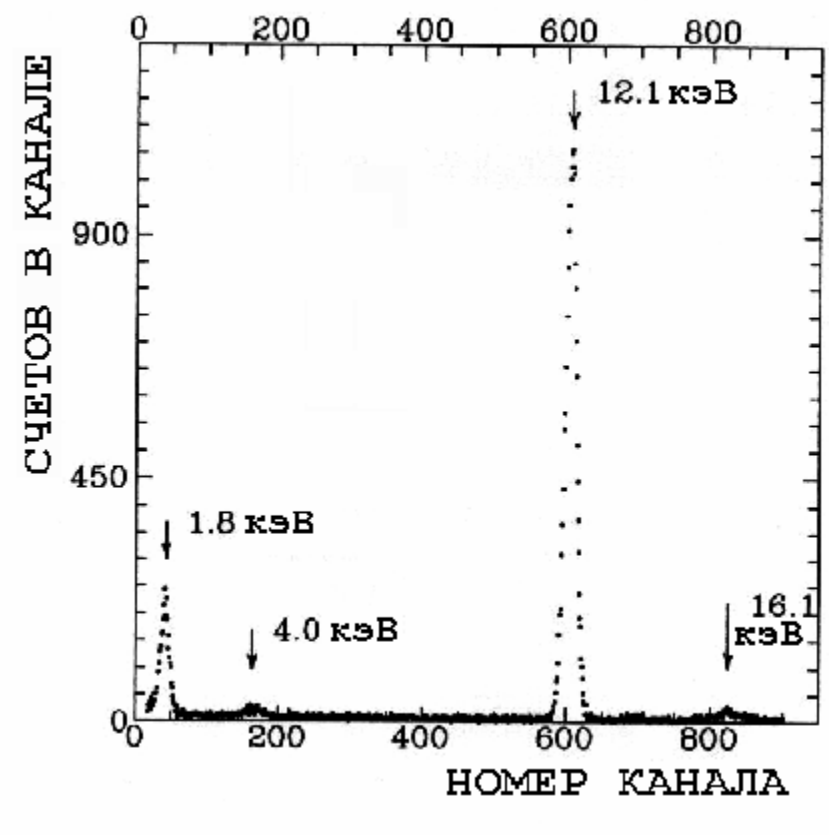

Спектры рентгеновского излучения измеренные при различных углах поворота мишени и энергии электронов 25.0 МэВ.

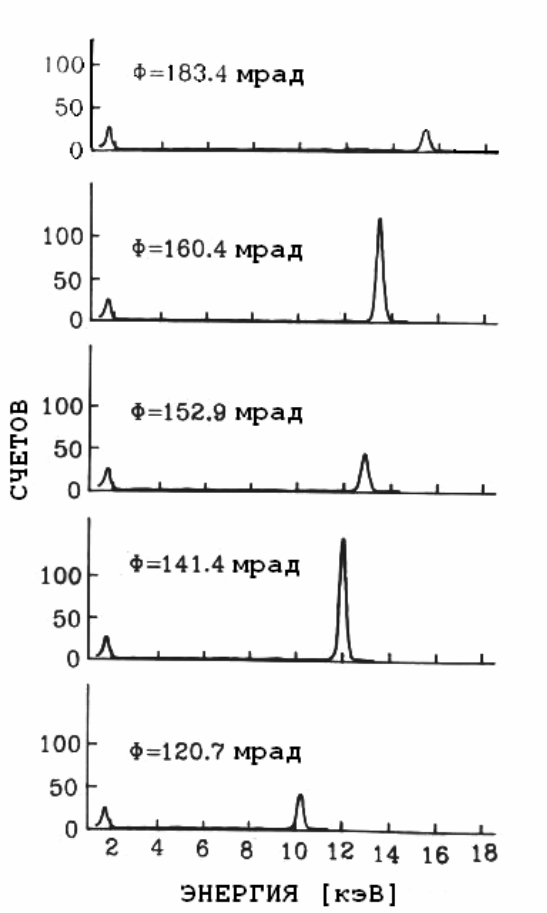

Энергии спектральных пиков в зависимости от угла поворота кристалла

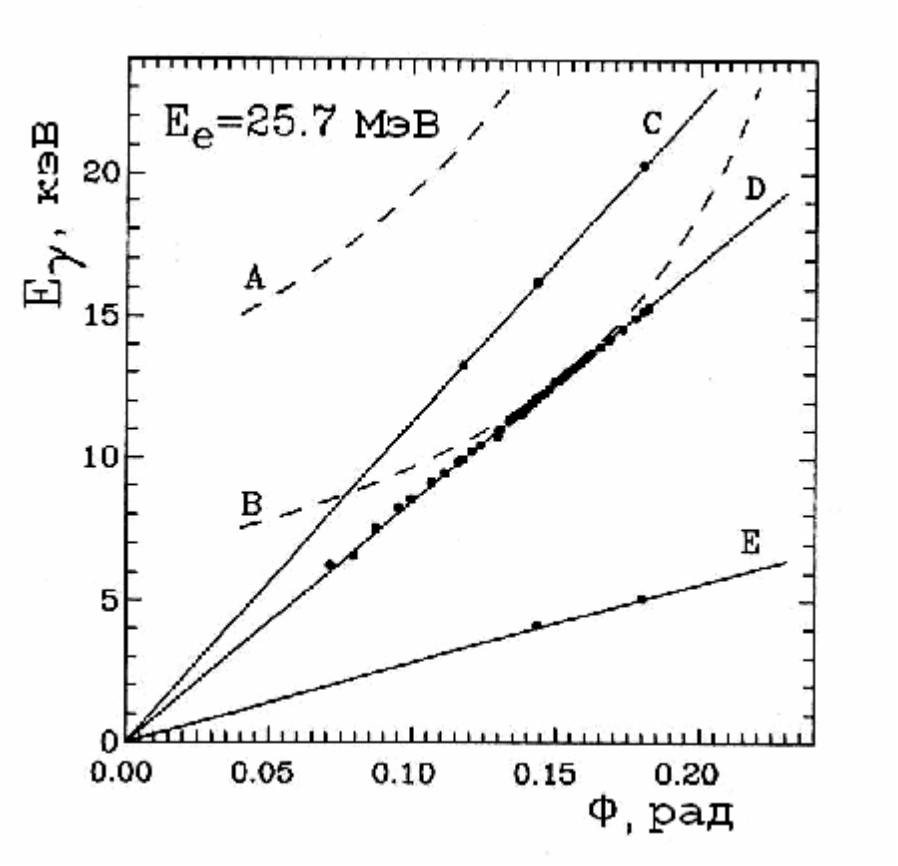

Эффект ряда для PXR.

Структура векторов обратной решетки монокристалла кремния в плоскости перпендикулярной вектору обратной решетки с индексами Миллера . (-220)

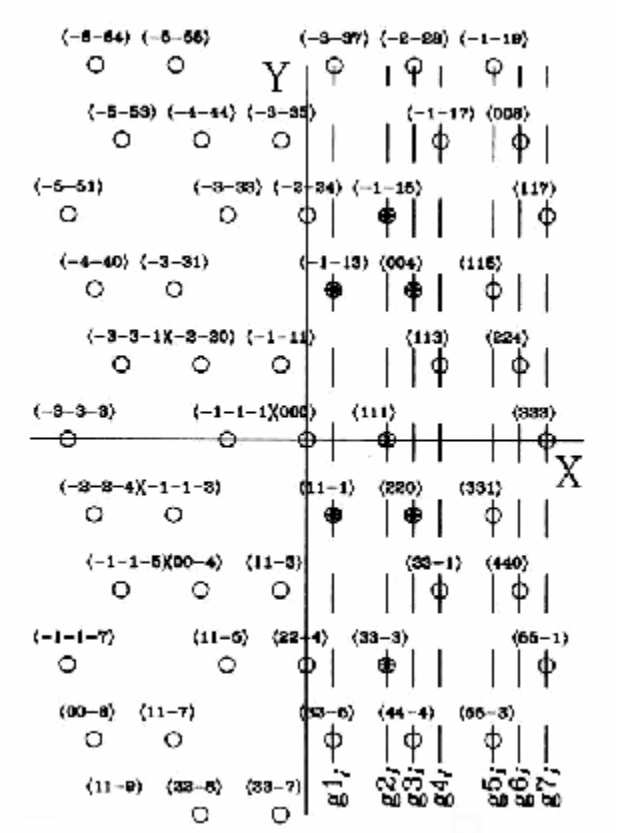

Абсолютный дифференциальный выход числа квантов ПРИ в спектральном пике вблизи рефлекса

Shchagin A.V., Khizhnyak N.A. Nucl. Instr. and Meth B 119, 115-122 (1996)

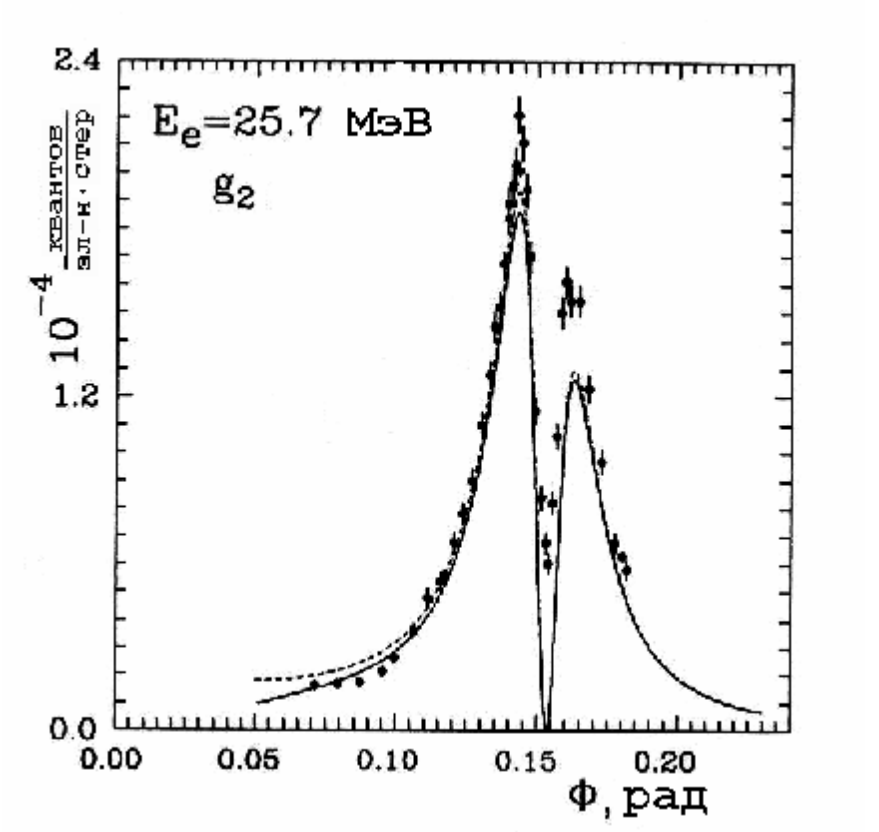

Абсолютный дифференциальный выход числа квантов ПРИ в спектральном пике вдали от рефлекса

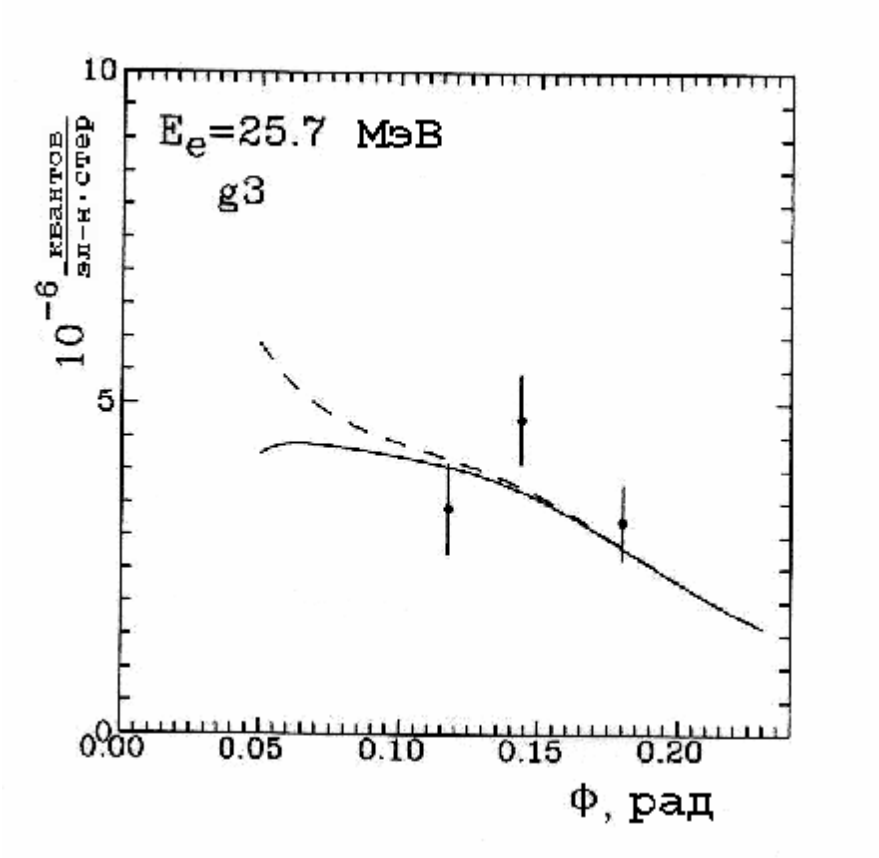

Угловое размер рефлекса ПРИ в зависимости от энергии электронов.

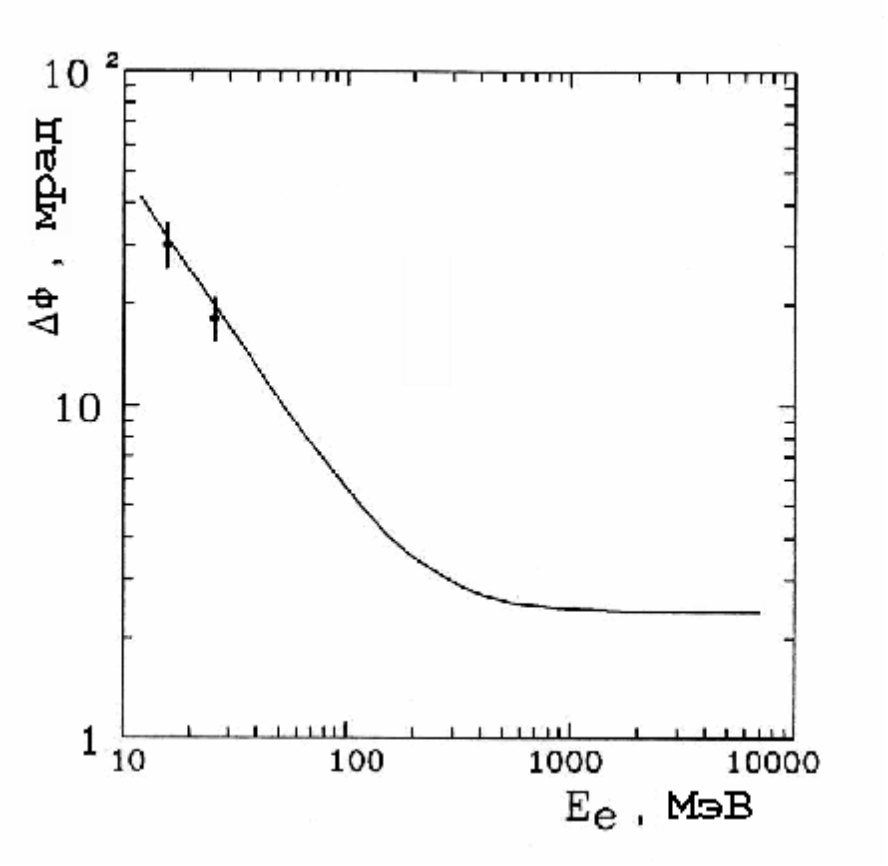

Дифференциальный выход ПРИ в левом и правом максимумах в зависимости от энергии электронов

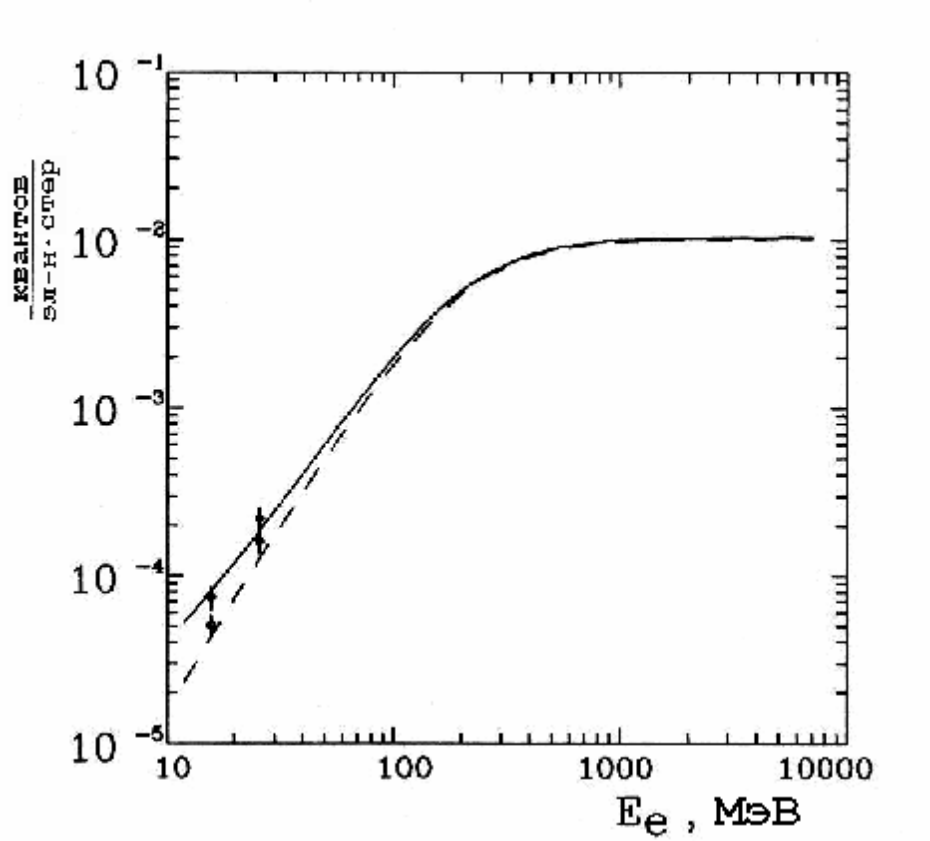

Angular distribution of the PXR yield at 90 degree. Fiorito R.B. et al, Phys. Rev. E 51, R2759-R2762 (1995).

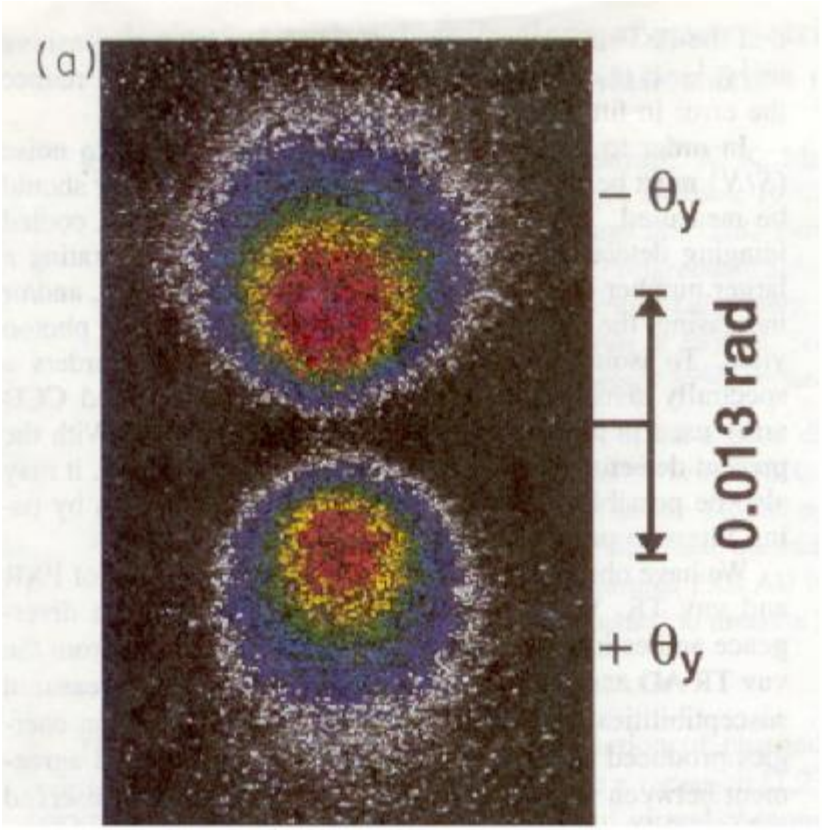

The setup for calibration of X-ray space telescopes at distance 518 m

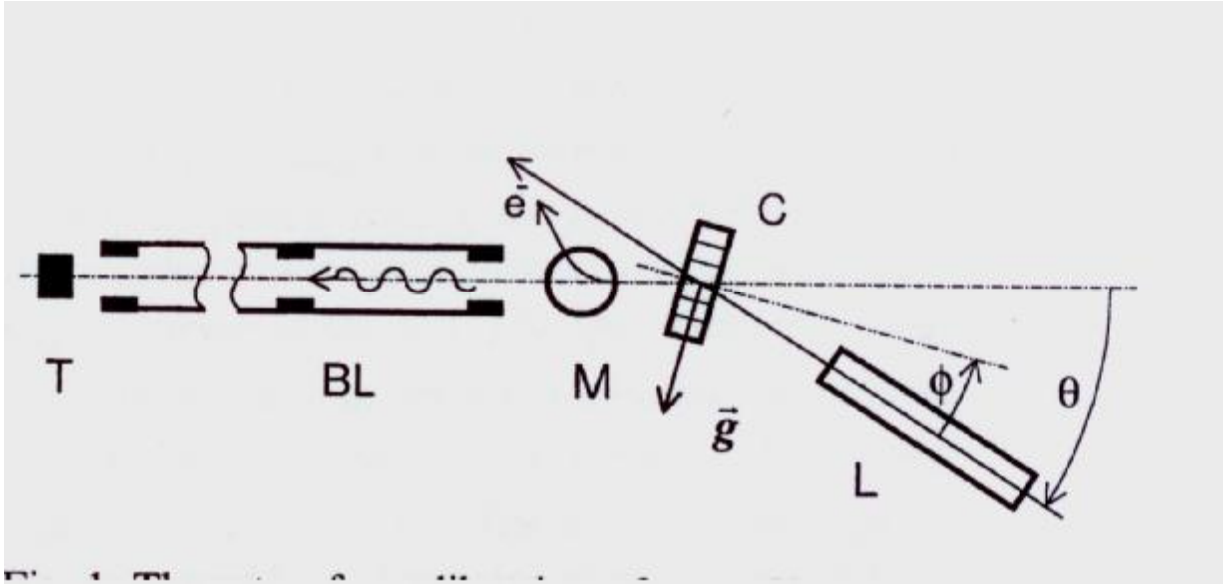

X-ray flux intensity at distance 518 meters

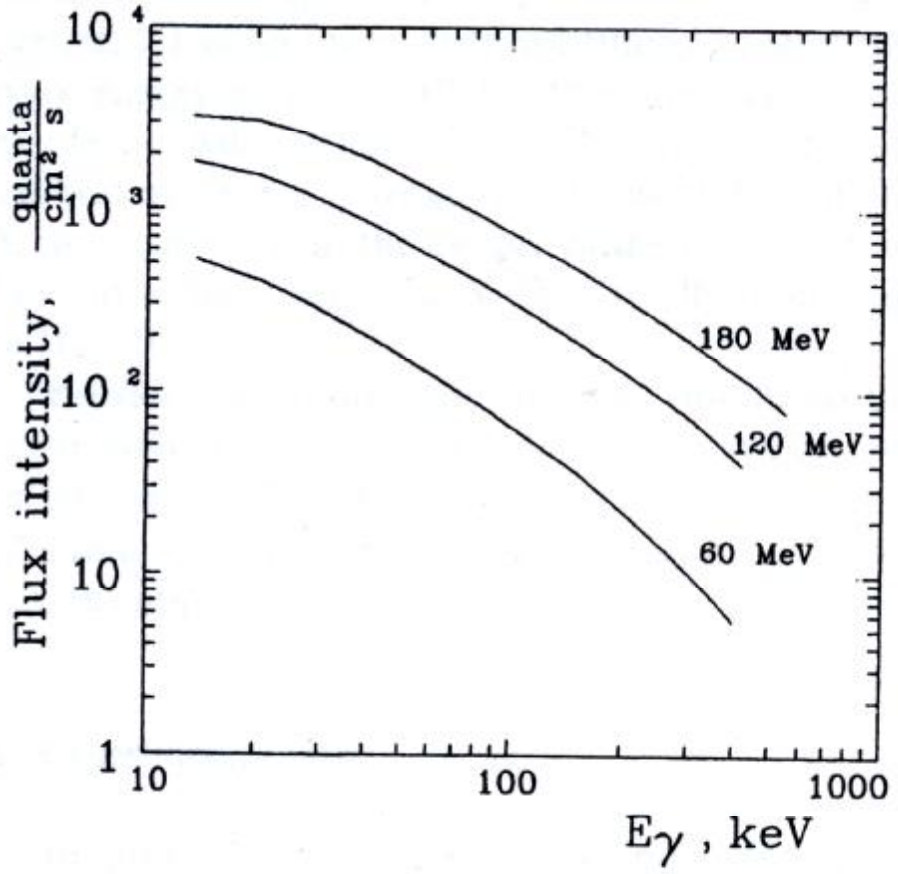

Fig. 2. X-ray flux intensity at the telescope aperture in units of quanta number per cm² per second as a function of quanta energy for incident electron energies of 60, 120 and 180 MeV.

X-ray locator based on the PXR for control of nuclear materials U, Pu

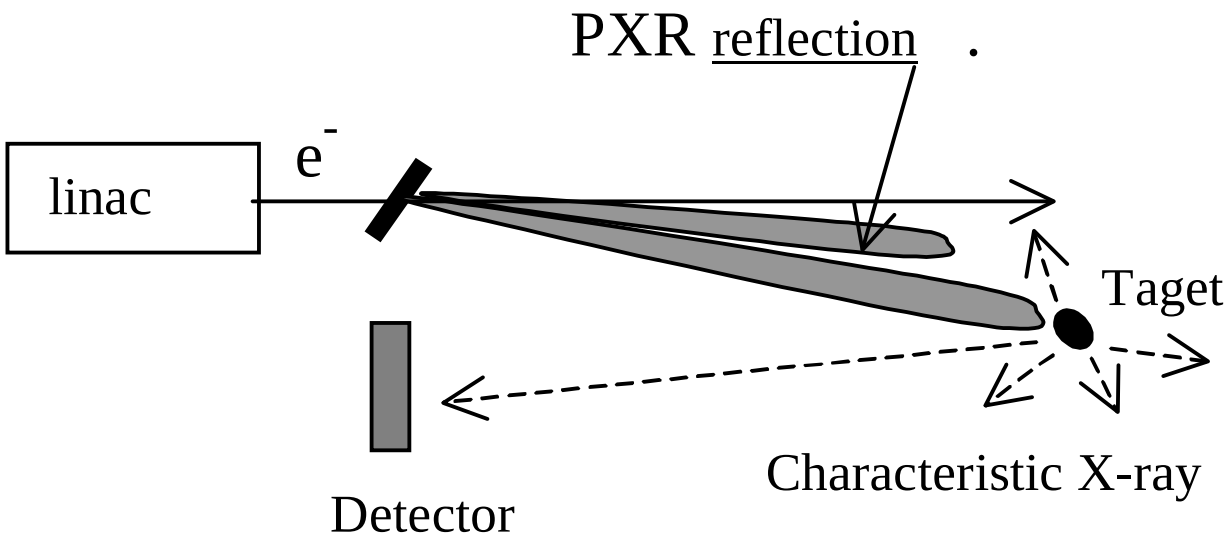

. The number of K characteristic quanta arriving in 1 sec at the 100 cm2 detector from the U target of area 1 cm2.

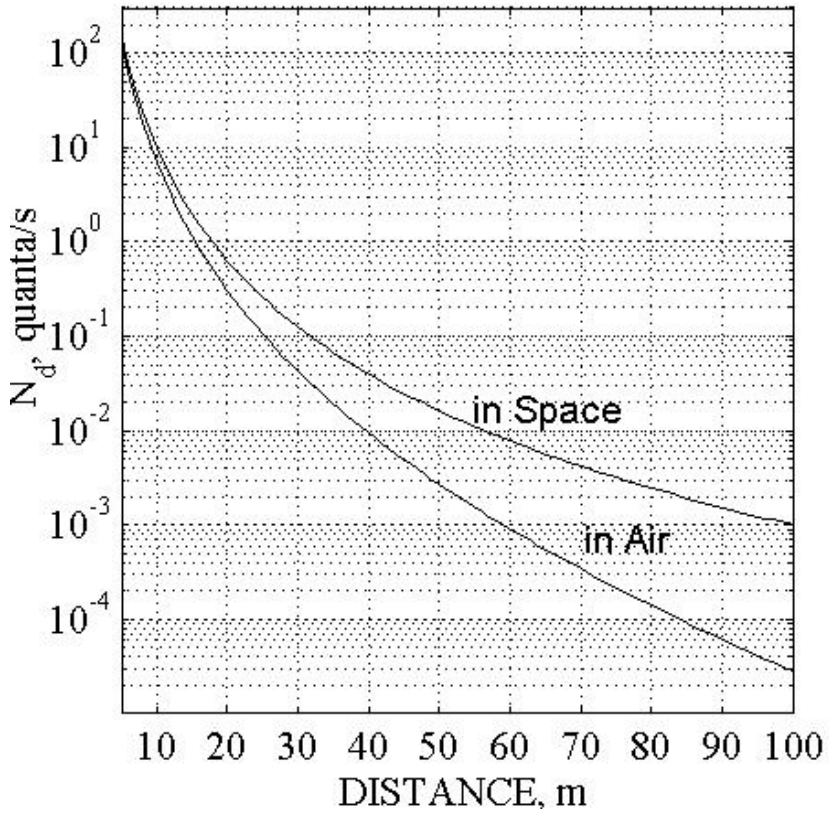

Production of PXR in a grain of a polycrystal. pA.V.

A.V. Shchagin, preprint http://arXiv.org/abs/physics/0105071 (2001); Вопросы атомной науки и техники. Серия «Плазменная электроника и новые методы ускорения» №4, 76-79 (2004).

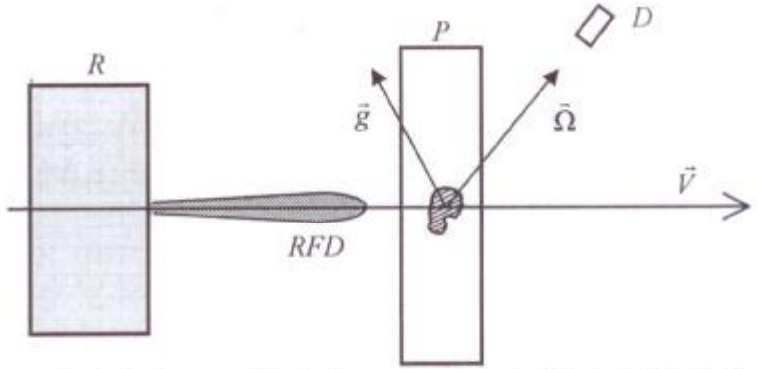

The relativistic particle beam passes through the radiator R and generates radiation in a forward direction (RFD). The RFD is going along the particle velocity vector $\vec{V}$ and passes through the polycrystalline foil P. One of randomly aligned grains of the polycrystal with the crystallographic planes and corresponding reciprocal vector $\vec{g}$ is shown in the foil. The spectrometric X-ray detector D is installed at observation angle θ relative to particle velocity vector. The observation direction is shown by the unit vector $\vec{\Omega}$. The detector can register RFD diffracted by polycrystal at Bragg energies

Experiment on PXR from textured polycrystal at 150 MeV
REFER ring at Hiroshima University

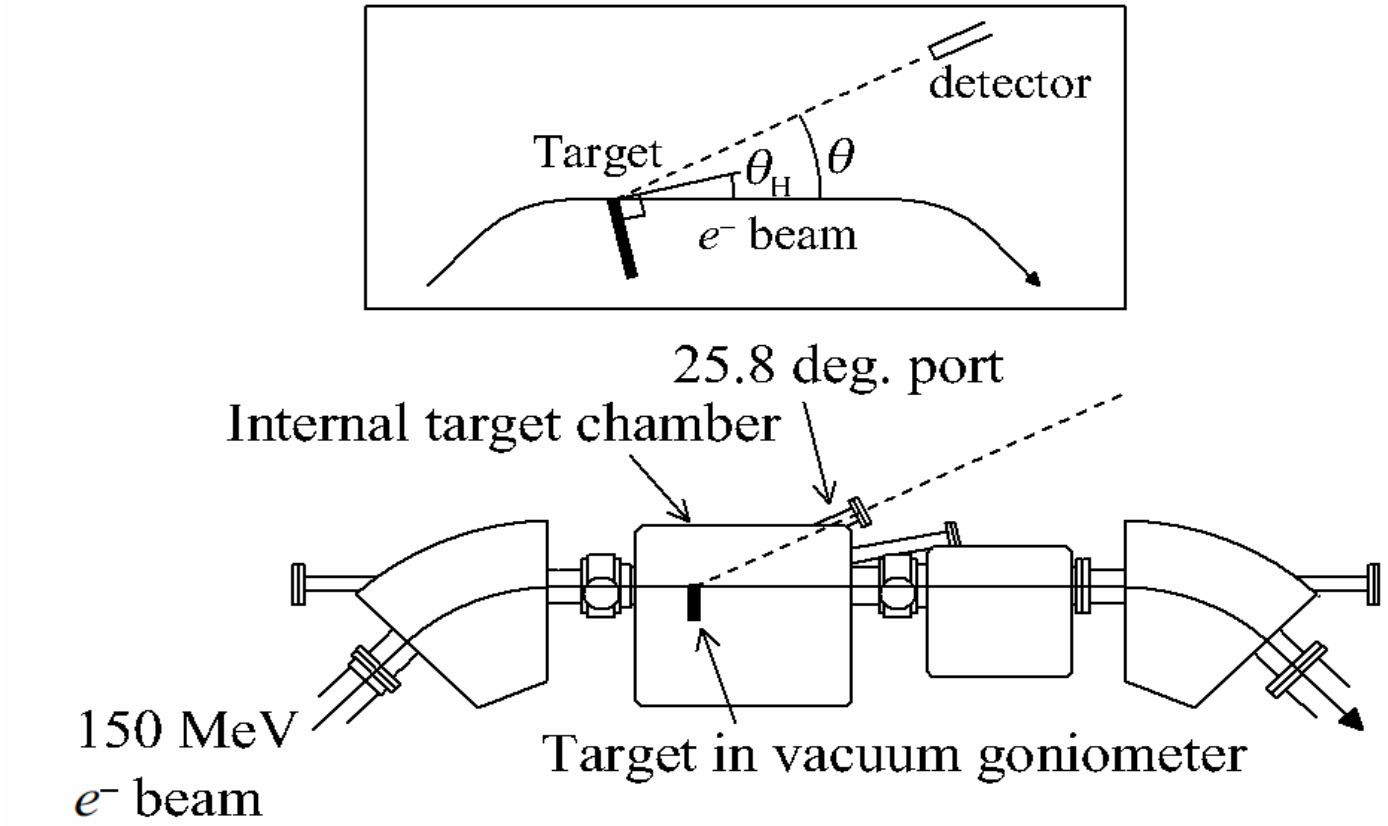

X-ray spectra from 10mkm thick Mo textured polycrystal. Y. Takabayashi, I. Endo, K. Weda, C. Moriyoshi, A.V. Shchagin,, NIMB B 243, 453-456 (2006).

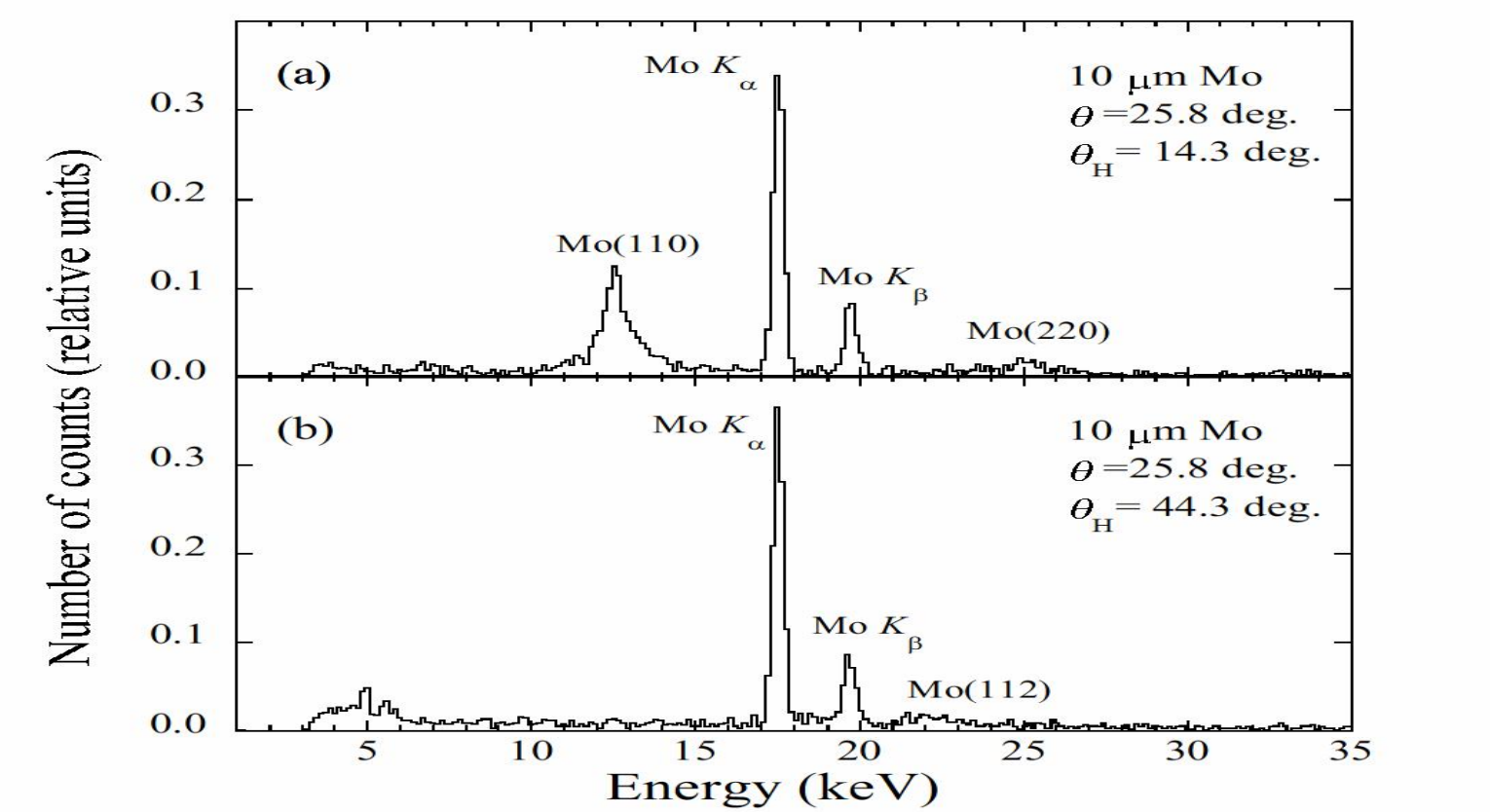

The yield and the spectral peak energy of PXR from textured Mo polycrystal

NIMB B 243, 453-456 (2006).

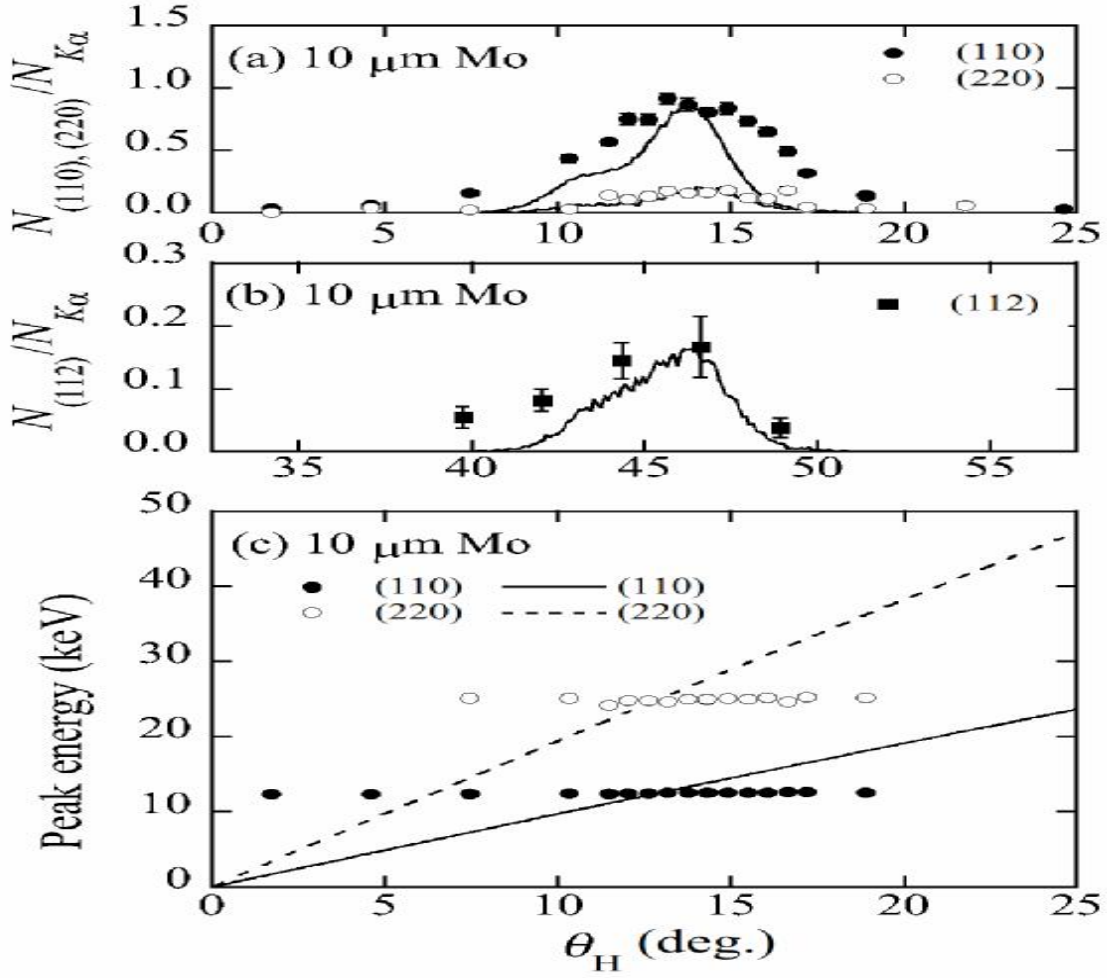

Intense PXR from textured polycrystal

S. Nawang[1], I. Endo[1], M. Iinuma[1], A. Kohara[1], H. Kuroiwa[2], C. Moriyoshi[3], T. Ohnishi[2], A. V. Schagin[4], S. Strokov[1], Y. Takabayashi[2], T. Takahashi[1], K. Ueda[1]

1) Graduated School of Advanced Sciences of Matter, Hiroshima University, Japan
2) Venture Business Laboratory, Hiroshima University, Japan
3) Graduated School of Science, Hiroshima University, Japan
4) Kharkov Institute of Physics and Technology, Ukraine

Background
- Observation of intense X ray from Molybdenum foil
  -- Mo foil ⟹ clear texture structure
- Few Systematic studies using textured polycrystal

Motivation
- Intense monochromatic X ray source for Medical application around 30-keV
- Clarification of basic properties of PXR from textured polycrystal

Purpose
- New systematic measurements at other observation angle
- Comparison with previous measurements, theory

REFER in Hiroshima University
(Relativistic Electron beam For Education and Research)

150 MeV Electron beam
Repetition : 10 Hz

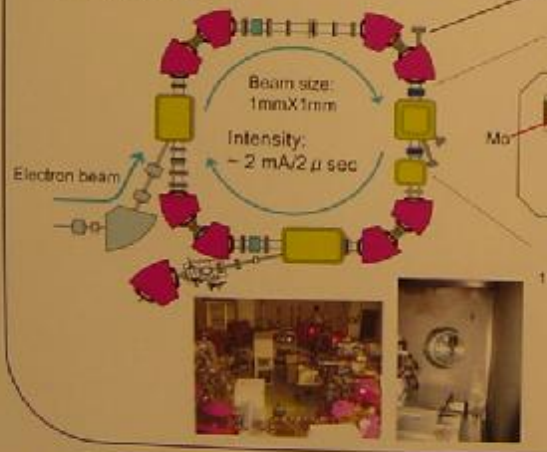

Experimental Setup

Observation angle :	Bragg angle
(θ_p)	(θ_B)
(1) 180 deg	90.0 deg
(2) 25.8 deg	12.9 deg
(3) 11.1 deg	5.55 deg

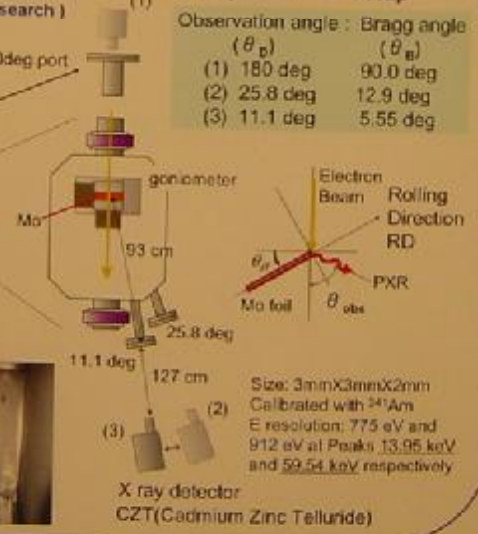

Size: 3mmX3mmX2mm
Calibrated with ^{241}Am
E resolution: 775 eV and 912 eV at Peaks 13.95 keV and 59.54 keV respectively

X ray detector
CZT(Cadmium Zinc Telluride)

Texture structure
(*10.0 μm* **Mo foil**)

Investigation by X ray diffraction independently

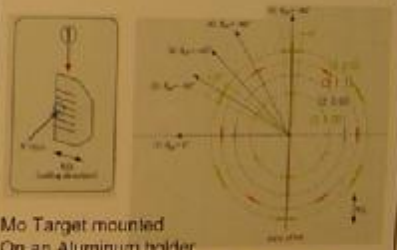

Mo Target mounted
On an Aluminum holder

JUL 26 2005

PXR Spectrum

Intensity and Energy
(θ = 25.8 deg.)

Intensity and Energy
(θ = 11.1 deg.)

(3) (2)

Calibrated with ^{241}Am
E resolution: 775 eV and 912 eV at Peaks 13.95 keV and 59.54 keV respectively

X ray detector
CZT(Cadmium Zinc Telluride)

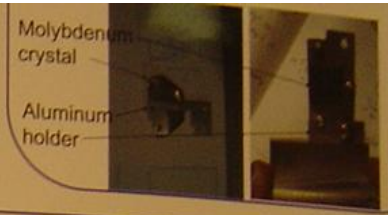

PXR Spectrum

Current Measurement

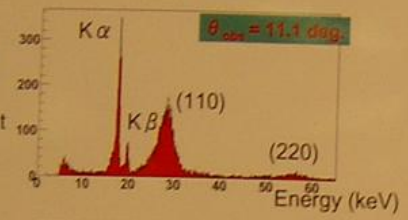

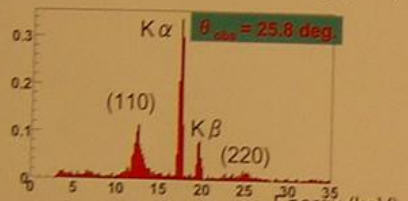

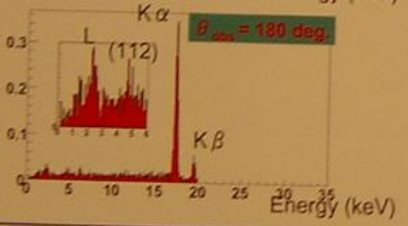

Intensity and Energy (θ = 25.8 deg.)

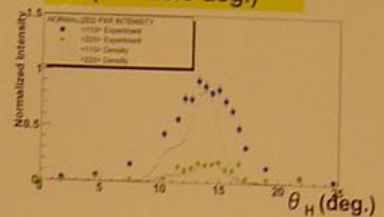

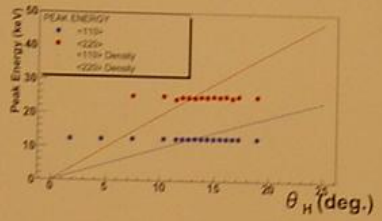

Intensity and Energy (θ = 11.1 deg.)

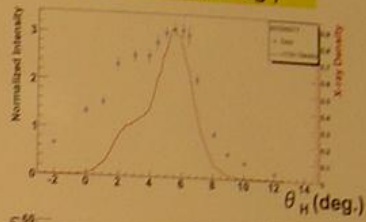

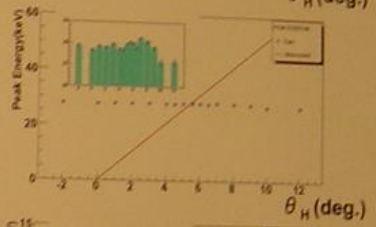

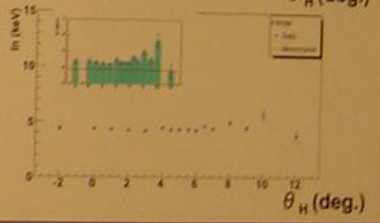

Intensity)

Angle (deg.)	Experimental Result
11.1	3.12±0.1
25.8	0.8±0.03
Ratio	3.9±0.24

Conclusion

- We obtained the Spectrum and extracted the Intensity and and Energy of PXR from textured polycrystal at various observation angles
- The x-ray energy depends on the observation angle only
- Medical Application around 30 keV looks promising.

JUL 26 2005

PXR may be extracted from long crystal.
Positive particle moves in channeling regime.
Multiple scattering is reduced

Fig

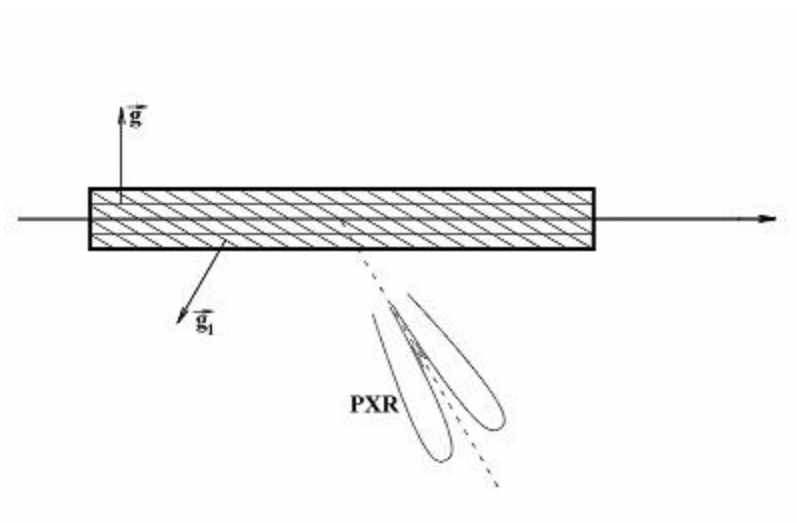

Production of focused PXR by particles channeling in a bent crystalline plate

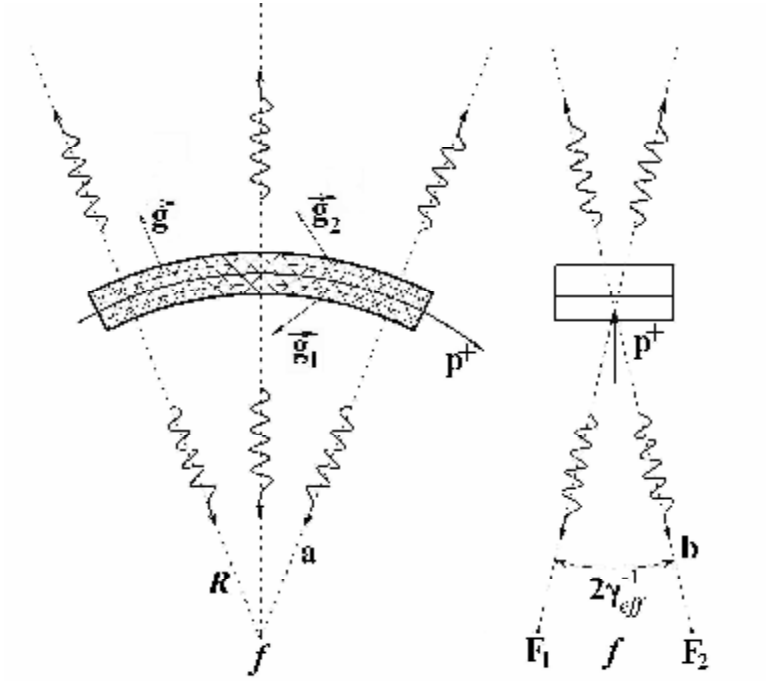

Production of focused PXR by particles channeling in a bent crystalline plate. The side and front views are shown in Figs. 1a and 1b, respectively. The particle beam is indicated by arrows p+. The particles are channeling along the crystallographic planes denoted by the reciprocal lattice vector g. The single-crystal plate is cylindrical in shape with a radius of curvature around the axis R. The wavy lines with arrows show the direction of radiation propagation at the maxima of the PXR reflections. The PXR reflections from the crystallographic planes denoted by the reciprocal lattice vector g1 are focused at points F1 and F2 on the axis f. The PXR focused at points F1 and F2 is linearly polarized practically in the plane of Fig. 1b.

The PXR reflections from the crystallographic planes denoted by the reciprocal lattice vector g2 are going in opposite directions and form virtual images of points F1 and F2.

The Huygens construction for focusing the PXR wave train

A.V. Shchagin, JETP Letters, 80, 535-540 (2004).

Fig

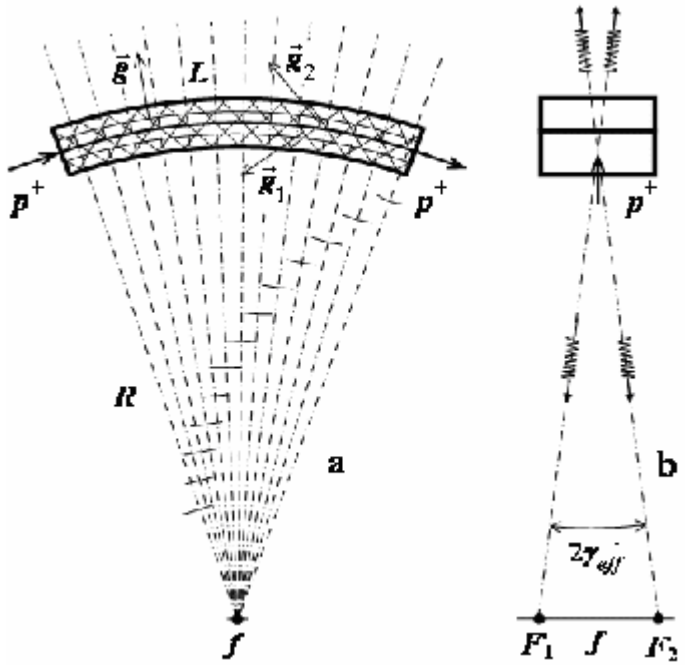

Properties of CXR and focused PXR induced by 70 and 450 GeV protons.

Si crystal size is 50*0.3 mm. X-ray detector square is 1 cm^2

Table

Radiation		CXR Si	PXR(400)	PXR(800)	PXR(12 00)
Polarization		No	Linear	Linear	Linear
$\overline{E}$, keV		1.74	6.46	12.91	19.37
$(\Delta E/E)_{nat}$			$3.84\cdot10^{-9}$	$1.92\cdot10^{-9}$	$1.28\cdot10^{-9}$
$(\Delta E/E)_{D}$			$2\cdot10^{-3}$	$2\cdot10^{-3}$	$2\cdot10^{-3}$
T_e in Si, μm		13.3	37	270	865
Protons 70 GeV	γ_{eff}^{-1}	-	$1.42\cdot10^{-2}$	$1.36\cdot10^{-2}$	$1.35\cdot10^{-2}$
	$\Delta F, mm$	-	142	136	135
	$I, \frac{quanta}{cm^2\cdot p^+}$	$1.65\cdot10^{-7}$	$9.56\cdot10^{-8}$	$1.86\cdot10^{-8}$	$1.55\cdot10^{-9}$
Protons 450 GeV	γ_{eff}^{-1}	-	$5.24\cdot10^{-3}$	$3.18\cdot10^{-3}$	$2.63\cdot10^{-3}$
	$\Delta F, mm$	-	52.4	31.8	26.3
	$I, \frac{quanta}{cm^2\cdot p^+}$	$1.94\cdot10^{-7}$	$6.90\cdot10^{-7}$	$3.32\cdot10^{-7}$	$3.98\cdot10^{-8}$

Diffraction and focusing of backward PXR

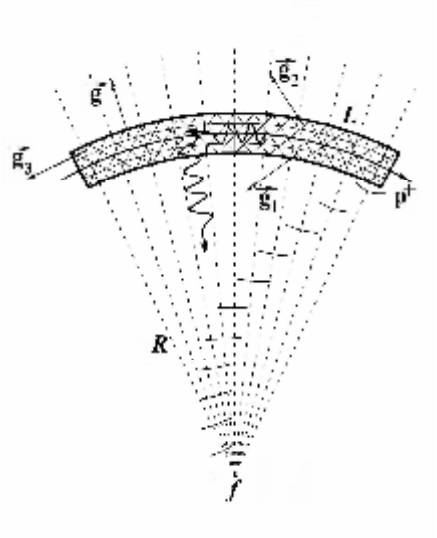

The backward-going PXR is generated on the crystallographic planes denoted by the reciprocal lattice vector g3. It is shown by a horizontal wavy line with the arrow. Then it is diffracted on the crystallographic planes denoted by the reciprocal lattice vector g2 and is focused at the axis f. The angular path before the diffraction is $g_{eff}^{-2}/2$ Shchagin, NATO ARW, Armenia 1994

Properties of diffracted and focused backward PXR induced by 70 and 450 GeV protons

Table

Radiation from $\vec{g}_3$	E, keV	Diffraction from $\vec{g}_2$	Protons 70 GeV $I, \frac{quanta}{cm^2 \cdot p^+}$	Protons 450 GeV $I, \frac{quanta}{cm^2 \cdot p^+}$
PXR($4\bar{4}0$)	6.46	($0\bar{4}0$)	$3.30 \cdot 10^{-15}$	$3.36 \cdot 10^{-8}$
PXR($8\bar{8}0$)	12.91	($0\bar{8}0$)	$3.86 \cdot 10^{-10}$	$3.56 \cdot 10^{-8}$
PXR($12\,\bar{12}\,0$)	19.37	($0\,\bar{12}\,0$)	$6.38 \cdot 10^{-11}$	$2.78 \cdot 10^{-8}$

Extraction of channeling radiation from a long crystal

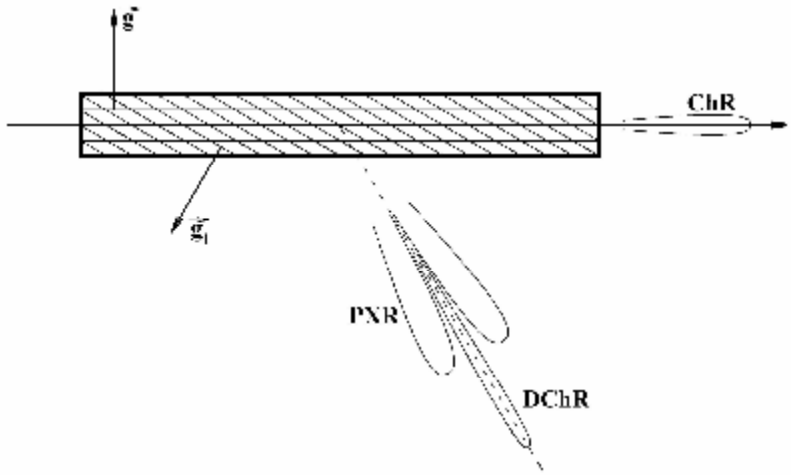

Positrons or other positive particles are channeling in a perfect crystal along the crystallographic planes denoted by the reciprocal lattice vector g. They emit channeling radiation (ChR) going along the particle trajectory. A part of the ChR of Bragg frequency is diffracted to the Bragg direction relative to the crystallographic planes denoted by the reciprocal lattice vector g1. The Bragg direction is shown by a dotted line. The angular distribution of ordinary PXR reflection is shown schematically around the Bragg direction. The angular distribution of diffracted and extracted DChR is shown along the Bragg direction.

The diffraction of channeling radiation was theoretically considered in: T. Ikeda, Y. Matsuda, H. Nitta, Y.H. Ohtsuki, Parametric X-ray radiation by relativistic channeled particles, Nucl. Instr. and Meth. B 115, 380-383 (1996).

Focusing of channeling radiation

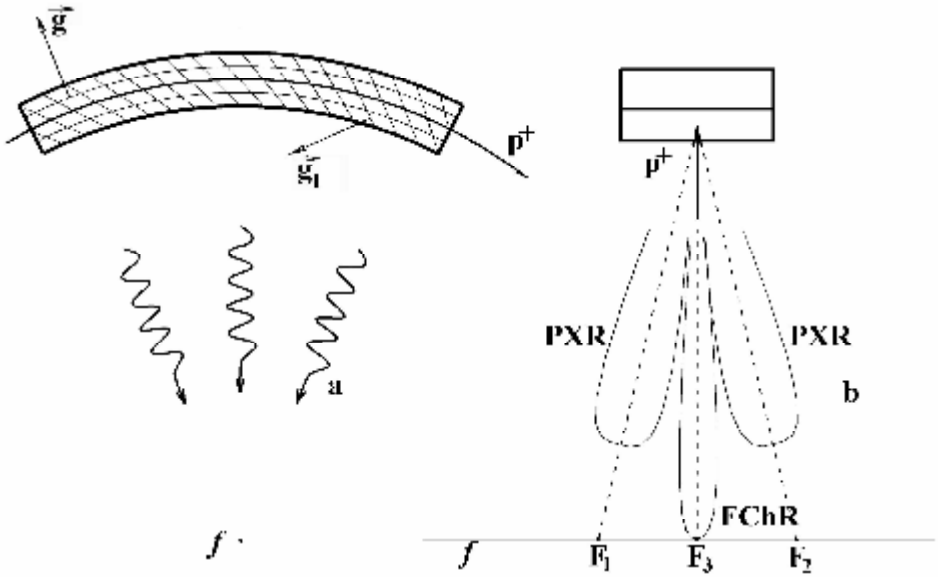

Focusing of channeling radiation. Positrons or other positive particles are channeling along the bent crystal in the crystallographic planes denoted by the reciprocal lattice vector g. They emit channeling radiation along of the particles trajectory. The diffracted at crystallographic planes denoted by reciprocal lattice vector g1 and extracted part of the channeling radiation (DChR) is focused at point F3. The ordinary PXR reflection is focused at points F1 and F2 just as in Fig. 1.

The PXR from a crystal undulator

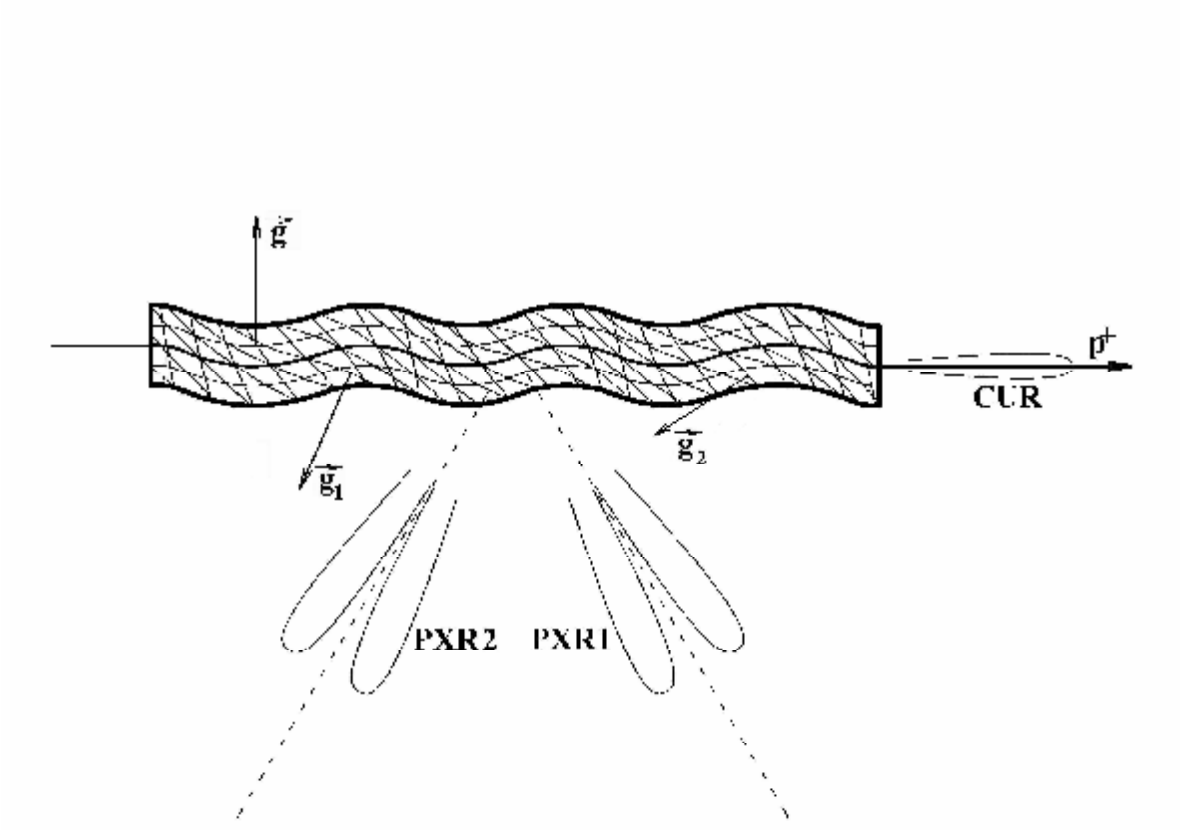

Generation of PXR reflections from the crystal undulator. The channeling particle emits crystal undulator radiation (CUR) in the forward direction. Besides, it emits PXR reflections in Bragg directions relative to different crystallographic planes of the crystal undulator. Only two sets of crystallographic planes denoted by the reciprocal lattice vectors g1 and g2 as well as the related Bragg directions and PXR reflections are shown in the figure.

Extraction of crystal undulator radiation

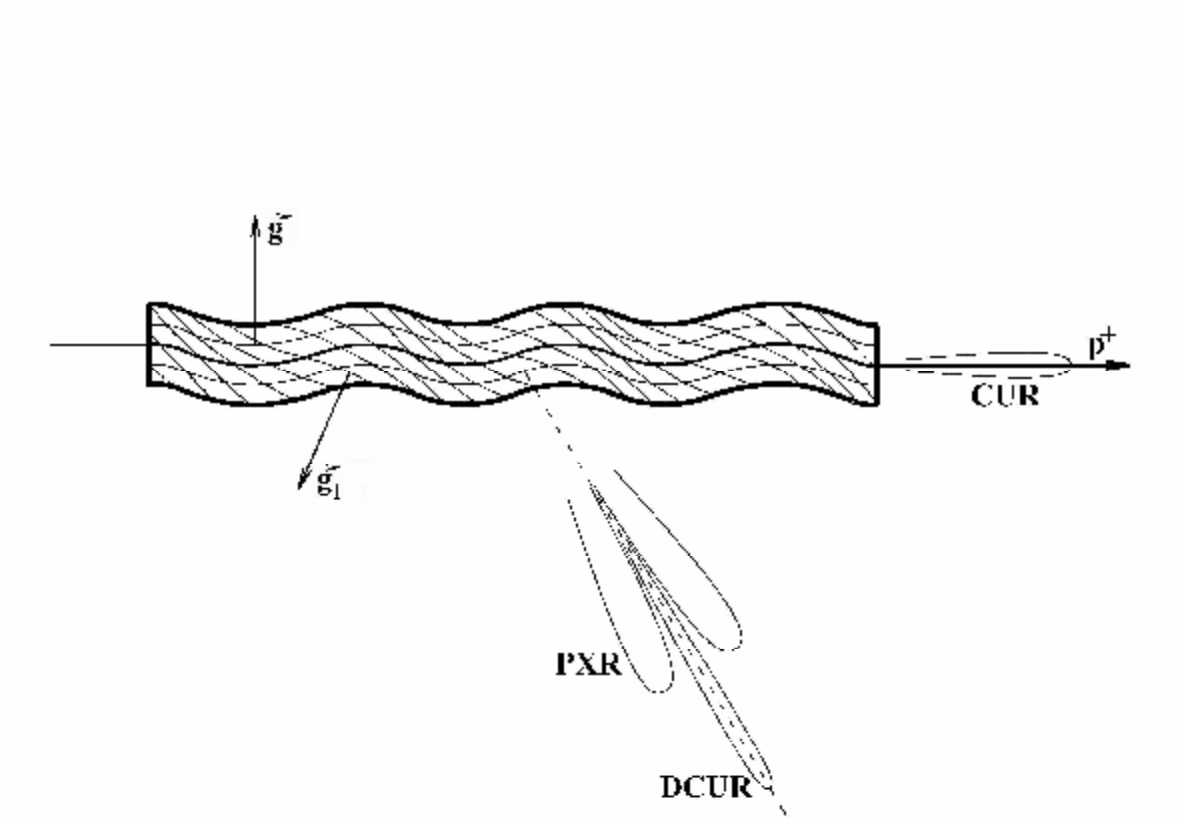

Extraction of undulator radiation from the crystalline undulator. The diffracted and extracted crystal undulator radiation (DCUR) is going along the Bragg direction. The PXR reflection is around the Bragg direction for the crystallographic planes denoted by the reciprocal lattice vector g1. The frequency of CUR should satisfy to Bragg condition for these crystallographic plane.

Focusing of crystal undulator radiation (CUR)

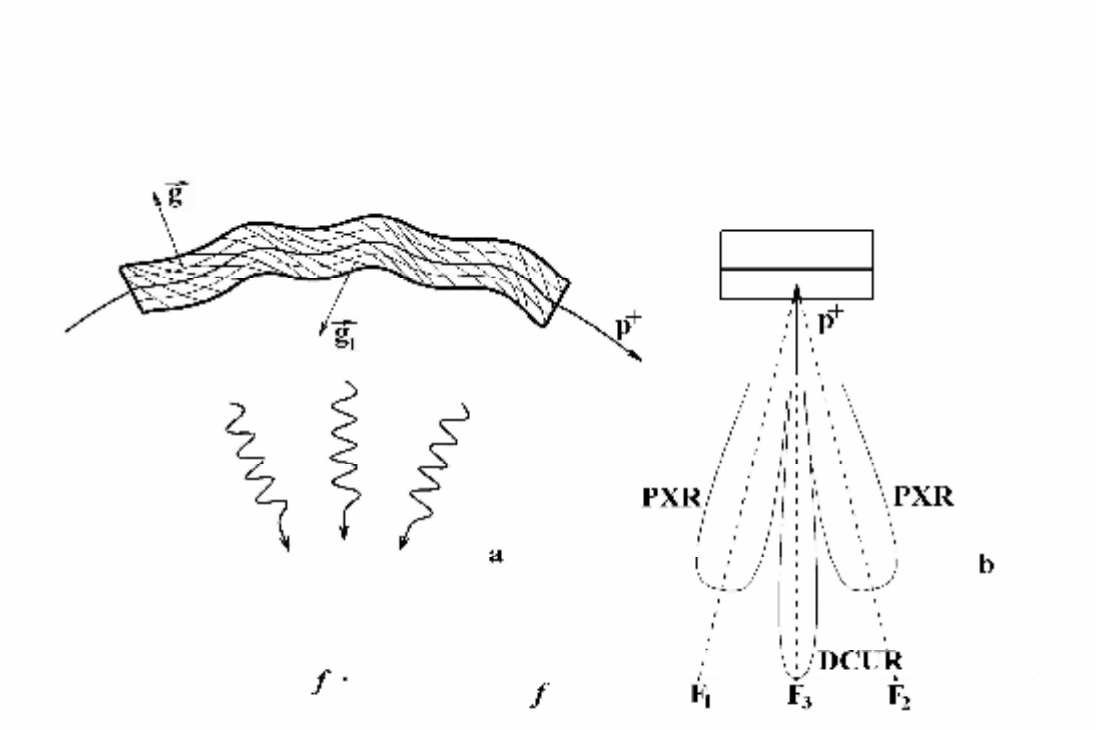

Diffraction, extraction and focusing of crystal undulator radiation. Positrons or other positive particles are channeling along a cylindrically bent crystal undulator in the crystallographic planes denoted by the reciprocal lattice vector g. They emit the CUR along of particles trajectory The diffracted and extracted part of the crystal undulator radiation (DCUR) is focused at the point F3 at axis f. The ordinary PXR reflection is focused at points F1 and F2 just as in Fig. 1. The CUR frequency should satisfy to Bragg condition.

The focused PXR train will possess the periodical frequency and phase modulation with the period determined by the crystal undulator period.

Applications of PXR in experiments with long crystal

1. **For high yield of PXR**
2. **For focusing of PXR**
3. **For proper alignment of the crystal undulator and for control and monitoring of the experiment**
4. **For focusing of channeling and undulator radiation**
5. **For generation of wavetrains with phase modulation**

Thanks
for Your Attention !